Feasibility Study on Stereotactic Radiotherapy for Total Pulmonary Vein Isolation in A Canine Model

Ji Hyun Chang
Seoul National University Hospital
Myung-Jin Cha (chamj81@gmail.com)
Seoul National University Hospital
Jeong-Wook Seo
Seoul National University Hospital
Hak Jae Kim
Seoul National University Hospital
So-Yeon Park
Veterans Health Service Medical Center
Byoung Hyuck Kim
Seoul Metropolitan Government-Seoul national university Boramae Medical Center
Euijae Lee
Sejong General Hospital
Moo-kang Kim
Seoul National University Hospital
Hye-sun Yoon
Seoul National University Hospital
Seil Oh
Seoul National University College of Medicine

Research Article

Keywords: atrial fibrillation, irradiation, pulmonary vein, cardiac radioablation, radiotherapy

Posted Date: December 31st, 2020

DOI: https://doi.org/10.21203/rs.3.rs-131387/v1

Feasibility study on stereotactic radiotherapy for total pulmonary vein isolation in a canine model

[1]Ji Hyun Chang, M.D., Ph.D, [2*]Myung-Jin Cha, M.D., [3]Jeong-Wook Seo, M.D., Ph.D, [1,4,5]Hak Jae Kim, M.D., Ph.D, [6,7]So-Yeon Park, Ph.D, [8]Byoung Hyuck Kim, M.D., Ph.D, [9]Euijae Lee, M.D., [2]Moo-kang Kim, B.S., [2]Hye-sun Yoon, B.S., [2,10]Seil Oh, M.D. Ph.D.

1 Department of Radiation Oncology, Seoul National University Hospital, Seoul, Republic of Korea

2 Division of Cardiology, Department of Internal Medicine, Seoul National University Hospital, Seoul, Republic of Korea

3 Department of Pathology, Seoul National University Hospital, Seoul, Republic of Korea

4 Department of Radiation Oncology, Seoul National University College of Medicine, Seoul, Republic of Korea

5 Cancer Research Institute, Seoul National University College of Medicine, Seoul, Korea

6 Department of Radiation Oncology, Veterans Health Service Medical Center, Seoul, Republic of Korea

7 Institute of Radiation Medicine, Seoul National University Medical Research Center, Seoul, Republic of Korea

8 Department of Radiation Oncology, Seoul Metropolitan Government-Seoul national university Boramae Medical Center, Seoul, Republic of Korea

9 Division of Cardiology, Department of Internal Medicine, Sejong General Hospital, Bucheon, Republic of Korea

10 Department of Internal Medicine, Seoul National University College of Medicine, Seoul, Republic of Korea

*Correspondence:

Myung-Jin Cha, M.D.

Assistant Professor of Internal Medicine,

Seoul National University Hospital,

101 Daehak-ro, Jongno-gu, Seoul 03080, Korea

Email: chamj81@gmail.com

Abstract

We tested the feasibility of pulmonary vein (PV) and left atrial (LA) posterior wall isolation using non-invasive stereotactic ablative body radiotherapy (SABR) and investigated pathological changes in irradiated lesions in a canine model. Seven male Mongrel dogs received single-fraction 33-Gy SABR. We designed the en-bloc circular target of total PVs and LA posterior wall to avoid the esophagus. The circular box lesion included the LA roof and ridge, low posterior wall, and posterior interatrial septum. At 6 weeks or 4 months post-SABR, electrical isolation of the SABR lesion was confirmed using LA posterior wall pacing, and histopathological review was performed. Electrical isolation of all PVs and the LA posterior wall was achieved in three of five dogs in the 4-month group. There was one target failure and one sudden death at 15 weeks. Although two dogs in the 6-week group failed to achieve electrical lesion isolation, the irradiated atrial myocardium showed diffuse hemorrhage with inflammatory cell infiltration. In successfully isolated 4-month model dogs, we observed transmural necrotic scarring with extensive fibrosis on irradiated atrial tissue. The findings suggest that this novel circular box-design radiotherapy technique using SABR could be applied to humans after further studies are conducted to confirm safety.

Keywords: atrial fibrillation, irradiation, pulmonary vein, cardiac radioablation, radiotherapy

Introduction

Atrial fibrillation (AF) is the most common cardiac arrhythmia, which increases the risk of stroke, hospitalization for heart failure, and death.[1] Catheter ablation is a well-established interventional approach for treating drug-refractory AF, but it is technically demanding, time-consuming, and invasive. Nevertheless, recurrence after catheter ablation occurs in at least 20% to 40% of patients, and there are complication risks related to the procedure in patients with advanced age or co-morbidities.[2,3] To overcome these limitations and invasiveness of the procedure, there is a need for a simple but effective delivery method. Recently, stereotactic radioablation has been suggested as a possible optional treatment for cardiac arrhythmias.[4]

The myocardial sleeve of the pulmonary vein (PV), which is known to be responsible for AF initiation, is the target of the ablation procedure.[5] Moreover, left atrial posterior wall isolation is known to reduce the recurrence of AF.[6] Therefore, the main treatment for AF ablation is electrical PV isolation (PVI) and posterior wall isolation (if needed) using an energy-delivery catheter technique. The objective of the AF ablation procedure is to create transmural, continuous, and permanent cellular damage in the targeted area.

Recently, stereotactic radioablation, which is known as stereotactic body radiotherapy or stereotactic ablative body radiotherapy (SABR) in the radiation oncology field, has shown great efficacy with acceptable toxicity in the treatment of refractory ventricular tachycardia (VT).[7] However, SABR for AF treatment has only been attempted on a very limited number of patients due to the close proximity of the PVs to other organs, especially the esophagus.[8,9] Previous *in vivo* animal studies on PVI with irradiation have shown the possibility of applying radiotherapy to PVI,[4,10-14] but these studies targeted only a single PV, which was the right superior PV ostium in most cases because of its sufficient size and study feasibility.

In the current study, we aimed to assess the feasibility of PV and posterior wall isolation using a SABR technique in a canine model.

Methods

Our experiments were approved by the Institutional Animal Care and Use Committee of Seoul National University Hospital (approved number: 18-0114-S1A1) and the animals were maintained in an Assessment and Accreditation of Laboratory Animal Care (AAALAC) international-accredited facility (#001169) in accordance with the Guide for the Care and Use of Laboratory Animals 8th edition.

Animals

Seven adult male Mongrel canines weighing 25–30 kg with baseline sinus rhythm were included in the study. A dog model was chosen since canine cardiac anatomy and electrophysiology are similar to that in humans, and as such, have been widely used in arrhythmia research.[15] Among them, three dogs were randomly selected for the persistent AF model. The other four dogs were assigned to the sinus rhythm model. Afterwards, one dog from the AF model and one dog from the sinus rhythm model were randomly selected to harvest at 6 weeks after irradiation and the remaining five dogs (two AF-model dogs and three sinus rhythm-model dogs) were harvested at 4 months. This study was carried out in compliance with the ARRIVE guidelines.[16]

Sinus rhythm and AF models

Dogs with sinus rhythm were monitored with an implantable loop recorder (Reveal LINQ™, Medtronic Inc., Minneapolis, MN, USA) to monitor cardiac rhythm. The AF burden before treatment was less than 0.1% of the total monitoring duration. Two dogs (4-month cases) could not be continuously monitored because of a technical problem.

Persistent AF was induced in three randomly chosen dogs using rapid atrial pacing of the left

atrial appendage for 1 month. The dogs were anesthetized and the chest was opened via minimal left thoracotomy at the fourth intercostal space. A bipolar screw-in pacing lead was fixed on the left atrial appendage via a minimal pericardial incision. The lead was then connected to a cardiac implantable electronic device (Unify Quadra™ or Promote™ RF; St. Jude Medical, Sylmar, CA, USA) placed in a pocket between the left chest muscle layers. The chest was closed, and the dog was allowed to recover for approximately 1 month before pacing was continued. Rapid atrial pacing was performed with 600 b.p.m. (pulse width 1.0 ms; 3.0 V) at 10 Hz. The dogs were followed on a weekly basis. The pacing was turned off and cardiac rhythm was checked to determine if the dog had developed AF. After 1 month of pacing, all three dogs developed AF that was sustained for more than 48 h. The dogs were observed for an additional 2 weeks before radiotherapy, and two of them were found to have sustained AF, but one dog was switched to the sinus rhythm model on the 7th day from pacing-off, and further rapid pacing for 7 days was performed.

Computed tomography (CT) simulation

Under general anesthesia, dogs were placed on a vacuum cushion in a prone position. In the first two dogs, immobilization using a thermoplastic mask was used; however, due to immobilization failure with the thermoplastic mask, the immobilization device was changed to a vacuum cushion. Contrast-enhanced CT simulation was performed after marking the reference point (1.8 ml/s, 80 ml, 10–12 sec). All dogs were scanned using the Brilliance CT Big Bore™ (Phillips, Cleveland, OH, USA). In dogs with a large respiratory amplitude (more than 5 mm), respiratory gated 10-phase four-dimensional (4D) CT images were acquired (RPM; Varian Medical Systems, Palo Alto, CA, USA). In dogs with a minimal respiratory amplitude less than 5 mm, a single-phase scan was performed. The slice thickness was 1 mm.

Target contouring and treatment planning

The SABR target for PVI was a “box lesion” in which all pulmonary veins as well as the posterior left atrial wall were encompassed by one large thick encircling belt lesion, which is used in all Maze procedures [17]. Largely, the target was delineated in two ways. First, in the initial two cases, the internal target volume (ITV) was delineated in a circle border-like donut shape at the LA wall that included four PV ostia inside the circle based on 4D-CT, and a 1-mm planning target volume (PTV) margin was added to the ITV (**Fig. 1A**). In these initial two cases (two dogs with sinus rhythm followed for either 6 weeks or 4 months), we experienced difficulties in cone beam CT (CBCT) matching because along with immobilization issues, uncertainty had increased because the ITV was confined to the LA wall and small PTV margin. Therefore, our subsequent target was made in a full circle-like shape, and a 4–5-mm margin was added to the PTV (**Fig. 1B**). Additionally, for CBCT matching, normal organs including the esophagus, trachea, bronchus, and pulmonary vessels were delineated.

Treatment planning was performed with Eclipse software (Varian Medical Systems, Palo Alto, CA, USA). The prescribed dose was 33 Gy in a single fraction. The main goal of the plan was to provide 100% volume of the PTV with administration of at least 99% of the prescribed dose.

Radiation treatment

SABR was delivered using TrueBeam™ (Varian Medical Systems, Palo Alto, CA, USA) under anesthesia. Thorough CBCT matching was performed for an alignment check before SABR.

Post-treatment electrophysiologic evaluation

After the planned time period (6 weeks or 4 months), all dogs were premedicated with tiletamine–zolazepam (Zoletil®; Virbac, Auckland, New Zealand) 5 mg/kg. After endotracheal intubation, general anesthesia was administered using isofluorane/O_2, and respiration was maintained with a mechanical ventilator. The chest was opened via a median sternotomy and the pericardium

incised. The right atrial appendage, left atrial appendage, and left atrial posterior wall were paced using two distal electrodes on a 5-Fr quadripolar electrophysiology catheter (Supreme™, St. Jude Medical, Minnesota, MN, USA). To capture the atrium, high-output pacing with a pacing cycle length of 1,000 msec was performed from 10 mA to 0.1 mA. A "box lesion" conduction block was defined when the atrium was not captured under supraphysiologic amplitude (five times the threshold of the left atrial appendage) [18]. The pacing test was conducted independently by two researchers (M.J.C and M.K.K).

One dog (sinus rhythm / 4-month) underwent pre- and post-radiotherapy electroanatomical 3-dimensional mapping of the left atrium using CARTO XP (Biosense Webster Inc., Diamond Bar, CA, USA). Using roving of the catheter tip, local electrical amplitudes were determined in the right upper PV antrum, proximal vein, and distal vein, and an electroanatomic voltage map was created. Voltage amplitudes of 1.0 mV indicated viable tissue. Voltages of 0.5 mV were considered representative of scar tissue. The proximal vein represented the target area for radiation.

Anatomical pathologic evaluation

Gross and microscopic pathology reviews were performed by a cardiac pathologist (J.W.S). After electrophysiological evaluation, the heart, including the pericardium, was explanted for gross examination. The heart and esophagus were stored in 10% formalin. Coronal or sagittal sectioned paraffin-embedded block tissue (size: 1 x 2 cm) was obtained from the targeted area with nearby tissue. Hematoxylin and eosin (H&E) and Masson's trichrome (MT) staining were performed for histopathological evaluation. Digital microscopic images were analyzed using Aperio Imagescope (Leica Biosystems, Buffalo Grove, IL, USA).

Results

Follow-up

Of the total seven dogs, six dogs survived until harvest day, but one dog died 1 week before its intended harvest day (sinus rhythm, 4-month follow-up model). An immediate autopsy was performed, and we found there was a scant amount of clear yellowish pericardial effusion without the pericardial tamponade feature. No evidence of coronary artery obstruction, perforation, intracardiac thrombus, or pulmonary embolism was observed. The diameter of the four cardiac chambers was within normal limits. The irradiated lesion was fibrotic, but the other part of atrium near the sinus or atrioventricular nodes was preserved. Cardiac rhythm was not monitored at that timepoint, and therefore, we could not determine the cause of sudden death.

Finally, we analyzed six dogs (two dogs with 6-week follow-up and four dogs with 4-month follow-up) for irradiated lesion isolation with pacing test. All six dogs maintained their initial rhythm until harvest. However, the AF burden of one dog in the AF group decreased from >99% to 83% after radiotherapy, although the AF burden of one dog with sinus rhythm increased from <1% to 3% after radiotherapy (**Fig. 2A**). The dogs with AF on the harvest day were switched to the sinus rhythm model with direct current cardioversion before the pacing test.

Pulmonary vein and left atrial posterior wall isolation

As demonstrated in **Table 1**, a conduction block from the left atrial posterior wall to the atrium was achieved in 0% (0/2) in the 6-week group and in 75% (3/4) in the 4-month group (except for the one dog that died suddenly). In three successful cases, pacing from the posterior wall inside the target lesion did not propagate outside the target area. The repeated pacing threshold test results showed that capture failure was confirmed inside the irradiated target area at 4 months (**Fig. 2B**). In the failed cases, the pacing threshold was higher in the AF model than the SR model. The one failed case in the 4-month group had undergone different radiotherapy planning, as described in the Methods section. The low voltage area indicating a scarred lesion on voltage mapping with the CARTO-3 electroanatomical mapping system (Biosense Webster Inc.) was consistent with the radiotherapy target area corresponding

to the planned target for irradiation (**Fig. 3A and 3B**).

Gross lesion and histopathological findings

The pericardial sac membranes of all seven dogs were thin and translucent, containing a scant amount of clear and serous fluid with no evidence of pericardial disease. The pericardial organs were visually intact without abnormal findings. There was no intracardiac thrombus in any of the seven dogs. The target adjacent structures such as the cardiac valves, esophagus, and aorta were intact in both the 6-week and 4-month groups (Supplementary Fig. S1 online).

There was no gross visual lesion on the target area at 6 weeks, but we definitely observed a transmural necrotic lesion in the area corresponding to the target area at 4 months (Supplementary Fig. S2 online), which also corresponded to the planned target lesion and low voltage area on electroanatomical mapping (**Fig. 3C and 3D**).

On the light microscopic evaluation at 6 weeks, compared to the adjacent myocardium outside the radiotherapy target lesion, sporadic vacuolization, diffuse hemorrhage, and inflammatory cell infiltration with dilated capillaries were observed (**Fig. 4**). On the light microscopic evaluation at 4 months, the target lesion was composed of massive hemorrhage with anucleated wavy fibers and extensive interstitial fibrosis (**Fig. 5**). The border zone between the target area and the unirradiated myocardium showed a mixture of viable myofibrils and fibrotic necrosis with extensive hemorrhage (Supplementary Fig. S3 online).

Discussion

To our knowledge, the present study is the first study to demonstrate the feasibility of total PV with LA posterior wall isolation with high-dose radiation in a large animal model. With a novel circular target design for SABR, the conduction block from the irradiated in-target area to the outside target was

completely achieved without capturing the atrial myocardium at 4 months, but not at 6 weeks. SABR targeting each of the four PVs would have increased uncertainty.

Recently, Monroy et al. and Qian et al. reported the human experience of non-invasive stereotactic radioablation for the treatment of atrial fibrillation.[19] In this study, two patients with drug-refractory AF were treated with radiation with 25-Gy single fraction. Although they reported no procedure-related complications, inevitable exposure to critical structures, such as the esophagus, may have been a major concern because AF is generally not directly related to sudden death. The ablation lesion set for AF treatment is complex, so this previous study was too small to reveal the feasibility or safety of cardiac radioablation for AF.

The optimal radiation dose for PV isolation is not currently established. In the previous animal study by Bode et al.,[12] using a porcine model, right superior pulmonary vein ablation was achieved using single 32.5-Gy radiotherapy. In another animal study by Zei et al., the right superior PVs of all 19 subjects (dogs or pigs) were treated with radiotherapy without complications at 35-Gy and 25-Gy with a partial effect at 20-Gy. Sharma et al.[20] reported that the voltage decreased at the left PV ostium in a study using 16 mini swine. The above human studies on two patients also applied 25 Gy based on the previous human VT trial.[21] The radiation dose used for the treatment of VT is 25-Gy in the clinical setting. However, the dose setting for AF needs to be considered because the antiarrhythmic mechanisms between the two treatments could be different. In VT, we have observed antiarrhythmic effects in the early phases after radiotherapy when fibrotic scars would not be present. In AF, however, it could be speculated that the fibrotic scar should be formed for PV isolation after catheter ablation. To determine the prescribed dose in the current study, we referred to the dose escalation study from Blanck et al., which showed doses >32.5 Gy could induce circumscribed scars.[11] Recently, Zei et al. reported that 25 Gy would be effective enough.[14] The goal of the current study was to assess the efficacy of SABR in AF treatment, and therefore, we selected a higher RT dose of 33 Gy than the dosage of 25 Gy used in VT treatment with SABR.

In human AF initiation and maintenance, the role of the PVs and LA posterior wall is well documented.[22] To treat human AF, the electrical isolation of total pulmonary veins from the left atrium is the standard treatment method. Atrioesophageal fistula or phrenic nerve palsy, which are two major complications related to AF ablation, may occur during ablation of the posterior parts of the LA [23]. Thus, we applied a modified circular box-lesion set anteriorly to all PVs and LA posterior wall. This novel target circular lesion included the posteroinferior part of the LA, part of the atrial septum, anterior LA roof, and the Coumadin ridge area between the LA appendage and the left PVs, which are traditional target areas for conventional AF ablation. We applied this design in both SR and AF models. The AF burden of one dog in the AF model was decreased after radiotherapy, although we could not verify whether this effect was a result of radiotherapy.

In the current study, we could not ensure the safety of radiotherapy for AF treatment. One dog with sinus rhythm without cardiac monitoring died suddenly. This occurred 3 days before the intended harvest day. Although we could not verify the cause of death from the autopsy results, the association between sudden death and radiotherapy cannot be ruled out. When we investigated the heart at autopsy, we could find any extensive transmural necrotic lesions across the atrium (Supplementary Fig. S4 online). Although the sinus or atrioventricular node area was visually and histopathologically preserved, it was possible that the intra- or inter-atrial conduction disturbance could lead to sudden bradyarrhythmia.

There are several limitations of this study to consider. First, we did not perform the irradiation in a sham-operated canine model as a control group. The reason for this was to minimize the number of sacrificed animals due to ethical considerations. Instead, we used the adjacent atrial myocardium in the same irradiated dog as a control part, which might be different to that of any control myocardium. However, we thought that this method was sufficient for lesion comparison because we were able to observe prominent differences between the two areas in all study subjects. Second, the canine cardiac structure is known to be different from that of human hearts. Although the heart size of a dog is similar to that of a human and most of the ion currents found in a human heart are present in a dog's heart, their

action potential shape and duration are known to vary. Most importantly, the anatomy of the pulmonary veins entering the LA is different in humans and dogs. For example, there are four pulmonary veins in humans, but 5~6 in dogs. In our study, the dogs also showed complex PV anatomy connected to the LA (Supplementary Fig. S5 online). Due to these anatomical variations, we experienced set-up errors as described in the Methods section. However, all cases with the modified RT design were successful in achieving block conduction. Considering the difficulties in the set-up process in dogs, it would be feasible to perform PV isolation in human with the designed SABR target. Third, we did not meticulously consider safety in the current experimental setting. Because dog atria are smaller than human atria and also ventrally elongated, the unwanted part of the right atrium was included in the target planning. We did not try to avoid the right atrium by minimizing the target volume. Although radiotherapy can successfully ablate the atrial myocardium, we should carefully consider the safety issue before applying this technique in human AF treatment. Lastly, we did not analyze the dose-responsiveness of the atrial myocardium from irradiation. There are very few studies in this field, so we focused on the feasibility of radioablation for AF. Further studies are needed to confirm the correct dose for safe radioablation.

In conclusion, all PVs and the LA posterior wall can be effectively isolated with a circular box-lesion ablated by radiotherapy (33-Gy, single fraction) in dog models. The conduction block was achieved in the 4-month model, and the irradiated lesion was definitely differentiated from the adjacent normal myocardium in the histopathological observation. This method could be applied to AF treatment with caution after further studies are conducted to ensure safety.

Data Availability Statement

The data underlying this article will be shared on reasonable request to the corresponding author.

References

1 Wang, T. J. *et al.* Temporal relations of atrial fibrillation and congestive heart failure and their joint influence on mortality: the Framingham Heart Study. *Circulation* **107**, 2920-2925, doi:10.1161/01.CIR.0000072767.89944.6E (2003).

2 Darby, A. E. Recurrent Atrial Fibrillation After Catheter Ablation: Considerations For Repeat Ablation And Strategies To Optimize Success. *J Atr Fibrillation* **9**, 1427, doi:10.4022/jafib.1427 (2016).

3 Steinbeck, G. *et al.* Incidence of complications related to catheter ablation of atrial fibrillation and atrial flutter: a nationwide in-hospital analysis of administrative data for Germany in 2014. *Eur Heart J* **39**, 4020-4029, doi:10.1093/eurheartj/ehy452 (2018).

4 Lehmann, H. I. *et al.* Feasibility Study on Cardiac Arrhythmia Ablation Using High-Energy Heavy Ion Beams. *Sci Rep* **6**, 38895, doi:10.1038/srep38895 (2016).

5 Khan, R. Identifying and understanding the role of pulmonary vein activity in atrial fibrillation. *Cardiovasc Res* **64**, 387-394, doi:10.1016/j.cardiores.2004.07.025 (2004).

6 He, X. *et al.* Left atrial posterior wall isolation reduces the recurrence of atrial fibrillation: a meta-analysis. *J Interv Card Electrophysiol* **46**, 267-274, doi:10.1007/s10840-016-0124-7 (2016).

7 Robinson, C. G. *et al.* Phase I/II Trial of Electrophysiology-Guided Noninvasive Cardiac Radioablation for Ventricular Tachycardia. *Circulation* **139**, 313-321, doi:10.1161/CIRCULATIONAHA.118.038261 (2019).

8 Shoji, M. *et al.* P4798Stereotactic radiotherapy for atrial fibrillation in three cancer patients. *European Heart Journal* **40**, doi:10.1093/eurheartj/ehz745.1174 (2019).

9 Monroy, E. *et al.* Late Gadolinium Enhancement Cardiac Magnetic Resonance Imaging Post-robotic Radiosurgical Pulmonary Vein Isolation (RRPVI): First Case in the World. *Cureus* **8**, e738-e738, doi:10.7759/cureus.738 (2016).

10 Sharma, A. *et al.* Noninvasive stereotactic radiosurgery (CyberHeart) for creation of ablation

lesions in the atrium. *Heart Rhythm* **7**, 802-810, doi:10.1016/j.hrthm.2010.02.010 (2010).

11 Blanck, O. *et al.* Dose-escalation study for cardiac radiosurgery in a porcine model. *Int J Radiat Oncol Biol Phys* **89**, 590-598, doi:10.1016/j.ijrobp.2014.02.036 (2014).

12 Bode, F. *et al.* Pulmonary vein isolation by radiosurgery: implications for non-invasive treatment of atrial fibrillation. *Europace* **17**, 1868-1874, doi:10.1093/europace/euu406 (2015).

13 Refaat, M. M. *et al.* Swine Atrioventricular Node Ablation Using Stereotactic Radiosurgery: Methods and In Vivo Feasibility Investigation for Catheter-Free Ablation of Cardiac Arrhythmias. *J Am Heart Assoc* **6**, doi:10.1161/JAHA.117.007193 (2017).

14 Zei, P. C., Wong, D., Gardner, E., Fogarty, T. & Maguire, P. Safety and efficacy of stereotactic radioablation targeting pulmonary vein tissues in an experimental model. *Heart Rhythm* **15**, 1420-1427, doi:10.1016/j.hrthm.2018.04.015 (2018).

15 Clauss, S. *et al.* Animal models of arrhythmia: classic electrophysiology to genetically modified large animals. *Nat Rev Cardiol* **16**, 457-475, doi:10.1038/s41569-019-0179-0 (2019).

16 Percie du Sert, N. *et al.* The ARRIVE guidelines 2.0: Updated guidelines for reporting animal research. *Journal of Cerebral Blood Flow & Metabolism* **40**, 1769-1777 (2020).

17 Cox, J. L. A brief overview of surgery for atrial fibrillation. *Ann Cardiothorac Surg* **3**, 80-88, doi:10.3978/j.issn.2225-319X.2014.01.05 (2014).

18 Hamner, C. E. *et al.* Irrigated radiofrequency ablation with transmurality feedback reliably produces Cox maze lesions in vivo. *Ann Thorac Surg* **80**, 2263-2270, doi:10.1016/j.athoracsur.2005.06.017 (2005).

19 Qian, P. C. *et al.* Noninvasive stereotactic radioablation for the treatment of atrial fibrillation: First-in-man experience. *J Arrhythm* **36**, 67-74, doi:10.1002/joa3.12283 (2020).

20 Sharma, A. *et al.* Noninvasive stereotactic radiosurgery (CyberHeart) for creation of ablation lesions in the atrium. *Heart Rhythm* **7**, 802-810, doi:https://doi.org/10.1016/j.hrthm.2010.02.010 (2010).

21 Cuculich, P. S. & Robinson, C. G. Noninvasive Ablation of Ventricular Tachycardia. *N Engl J*

Med **378**, 1651-1652, doi:10.1056/NEJMc1802625 (2018).

22 Oral, H. *et al.* Pulmonary vein isolation for paroxysmal and persistent atrial fibrillation. *Circulation* **105**, 1077-1081 (2002).

23 Pappone, C. *et al.* Atrio-esophageal fistula as a complication of percutaneous transcatheter ablation of atrial fibrillation. *Circulation* **109**, 2724-2726 (2004).

Acknowledgements

This work was supported by a National Research Foundation (NRF) of Korea grant funded by the Korean government (No. NRF-2020R1A2C1013832) from MJ Cha and also supported by the National Research Foundation (NRF) funded by the Ministry of Science & ICT (NRF-2018M2A2B3A01070410) from JH Chang.

Author contributions

JH Chang and M Cha conceived of the presented idea, planned the study, derived the models and analyzed the data, wrote the main manuscript text and prepared figures. HJ Kim, S Park, BH Kim carried out the experiments, aided in interpreting the results and worked on the manuscript. E Lee, M Kim, and H Yoon designed and carried out the experiments, derived the models, analyzed the data, and prepared figures. JW Seo and S Oh verified the analytical methods, and supervised the findings of this work. All authors reviewed the manuscript, discussed the results and commented on the manuscript.

Competing Interests

The authors declare no competing interests.

Figure legends

Figure 1. Radiotherapy design. A. Axial (**a**) and sagittal (**b**) view of simulation CT (left), dose distribution with isodose lines (middle), and cone beam CT for set-up verification (right). Red, target; cyan, planned target volume (PTV); yellow, pulmonary veins; light green, left atrium. B. Posterolateral view of 3D reconstructed contoured target. CT, computed tomography; LA, left atrium; PV, pulmonary vein

Figure 2. Post-radiotherapy cardiac rhythm and electrophysiologic evaluation. a. Among the three dogs with 100% burden of atrial fibrillation (AF), AF burden is decreased to 83% of that during cardiac monitoring in one dog. The initial AF burden (100%) is maintained in the other two dogs. Among the four dogs with normal sinus rhythm (SR) without AF at baseline, SR is maintained in two dogs, but 3% AF burden is maintained in one dog after irradiation.b. Atrial pacing tests confirmed that pacing was not captured inside the irradiated target area at 4 months

LAA, left atrial appendage; RAA, right atrial appendage

Figure 3. Myocardial necrotic scar formation on irradiated left atrial posterior wall. The reconstructed target area from the posterior view (white arrows in **a**) corresponds with the low voltage area (red area with white arrows in **b**) indicating a scarred lesion on voltage mapping with the CARTO-3 electroanatomical mapping system (Biosense Webster Inc.). The targeted lesion is grossly distinguishable at 4 months from both the epicardial (**c**) and endocardial (**d**) side.

Figure 4. Histologic changes after irradiation at 6 weeks. There is no gross lesion at 6 weeks. However, from the light microscopic evaluation with H&E and MT staining, compared to normal atrial myocardium near the irradiated lesion (**a**), irradiated atrial myocardium (**b**) shows diffuse vacuolization with extensive hemorrhage and inflammatory cell infiltration with dilated capillaries. H&E, hematoxylin and eosin; MT, Masson's trichrome

Figure 5. Histologic changes after irradiation observed at 4 months. A visually definite transmural

necrotic lesion is observed on the irradiated area at 4 months. Compared to the normal atrial myocardium near the irradiated lesion (**a**), irradiated atrial myocardium (**b**) shows massive hemorrhage with anucleated wavy fibers with extensive interstitial fibrosis. H&E, hematoxylin and eosin; MT, Masson's trichrome

Table 1. Study results

Follow-up		Cardiac rhythm		Pacing threshold (mA)*		Study result	
	Initial	Harvest day	Inside IR lesion (LA posterior wall) (**A**)	Left atrial appendage (**B**)	Right atrial appendage	**A/B**	
6 weeks	SR	SR	0.8	0.8	0.8	1	Fail
6 weeks	AF	AF†	1.6	1.8	0.8	0.89	Fail
4 months	SR	SR	> 10	0.2	0.2	> 50	Fail
4 months	SR	-	-	-	-		N/A
4 months	SR	SR	> 10	0.8	0.8	> 12.5	Success
4 months	AF	AF†	10	1.4	1.0	7.14	Success
4 months	AF	AF†	8	0.8	1.0	10	Success

* Pulse width 1.0 ms

† Pacing threshold test was performed under sinus rhythm after direct current cardioversion

SR, sinus rhythm; AF, atrial fibrillation; IR, irradiated; LA, left atrial; N/A, not applicable

Figures

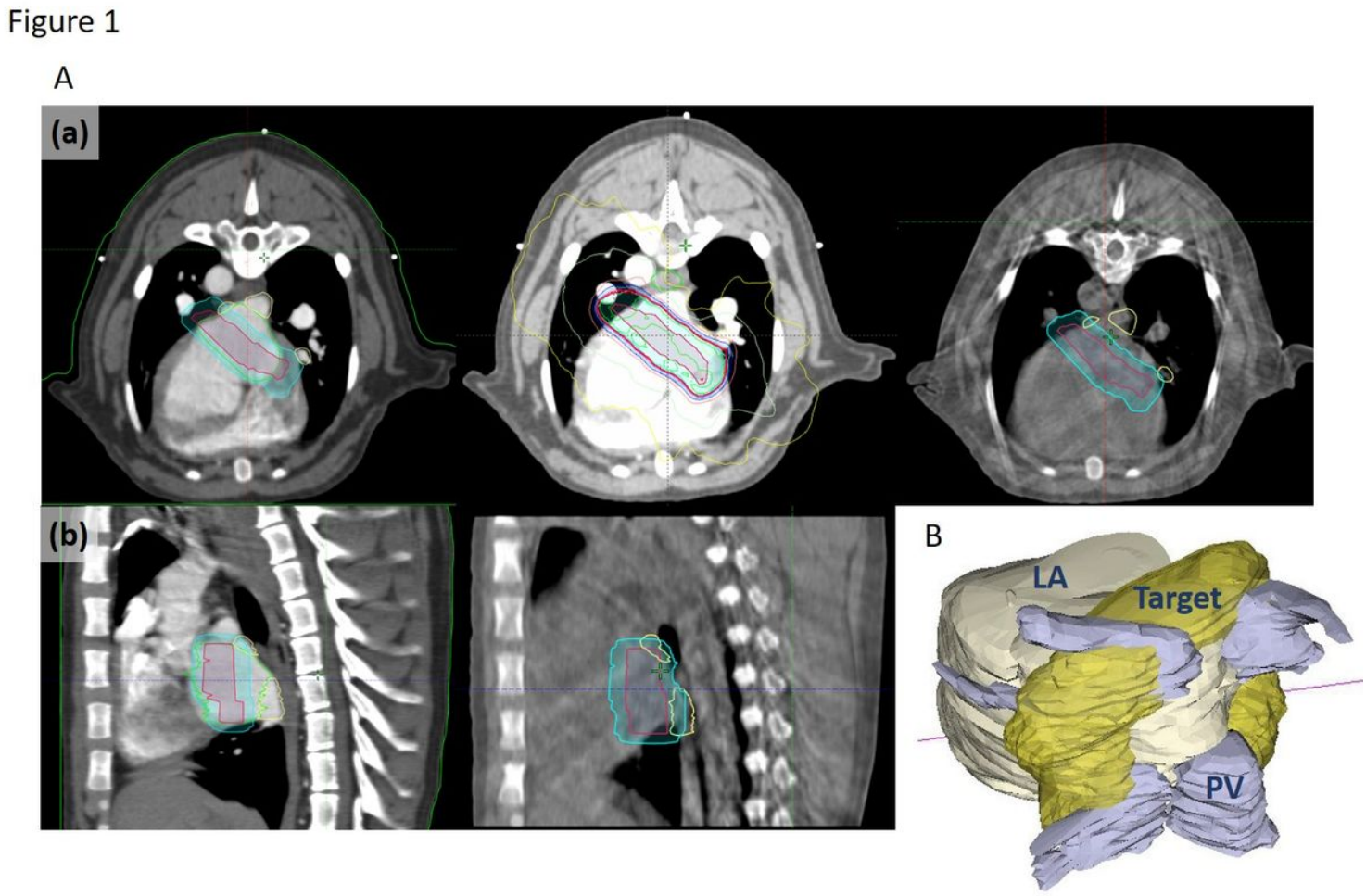

Figure 1

Radiotherapy design. A. Axial (a) and sagittal (b) view of simulation CT (left), dose distribution with isodose lines (middle), and cone beam CT for set-up verification (right). Red, target; cyan, planned target volume (PTV); yellow, pulmonary veins; light green, left atrium. B. Posterolateral view of 3D reconstructed contoured target. CT, computed tomography; LA, left atrium; PV, pulmonary vein

Figure 2

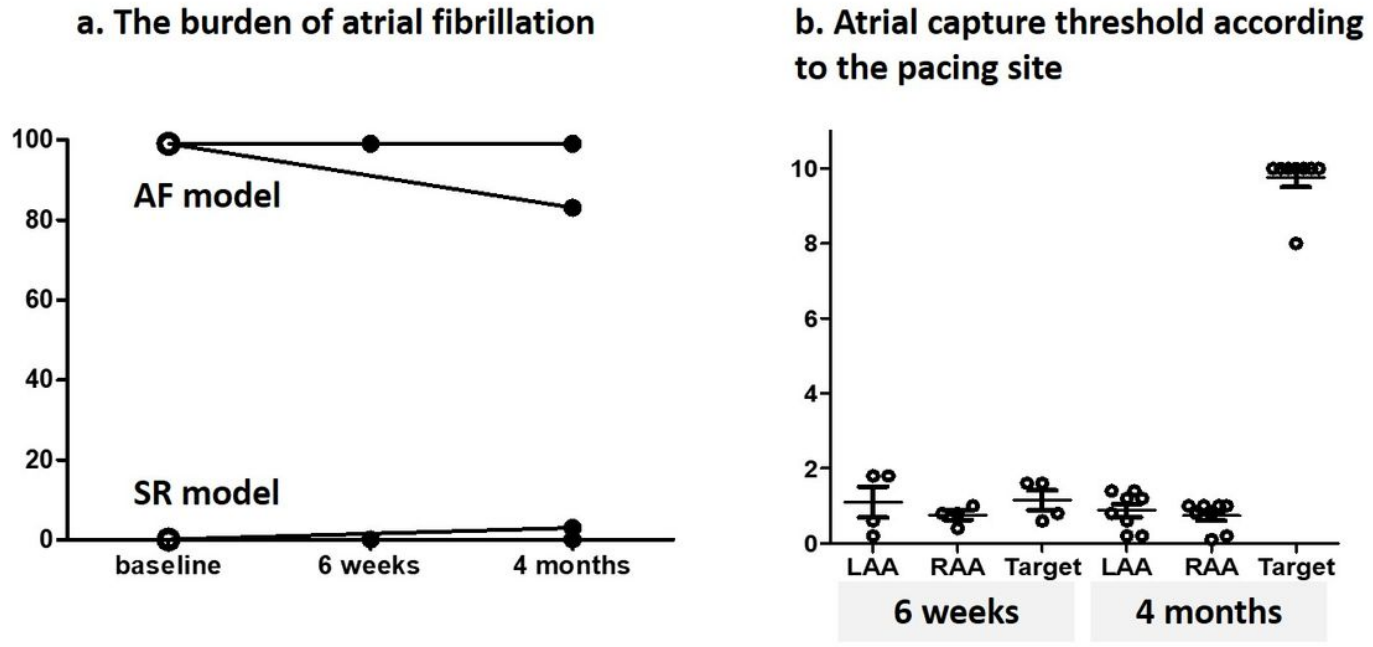

Figure 2

Post-radiotherapy cardiac rhythm and electrophysiologic evaluation. a. Among the three dogs with 100% burden of atrial fibrillation (AF), AF burden is decreased to 83% of that during cardiac monitoring in one dog. The initial AF burden (100%) is maintained in the other two dogs. Among the four dogs with normal sinus rhythm (SR) without AF at baseline, SR is maintained in two dogs, but 3% AF burden is maintained in one dog after irradiation.b. Atrial pacing tests confirmed that pacing was not captured inside the irradiated target area at 4 months LAA, left atrial appendage; RAA, right atrial appendage

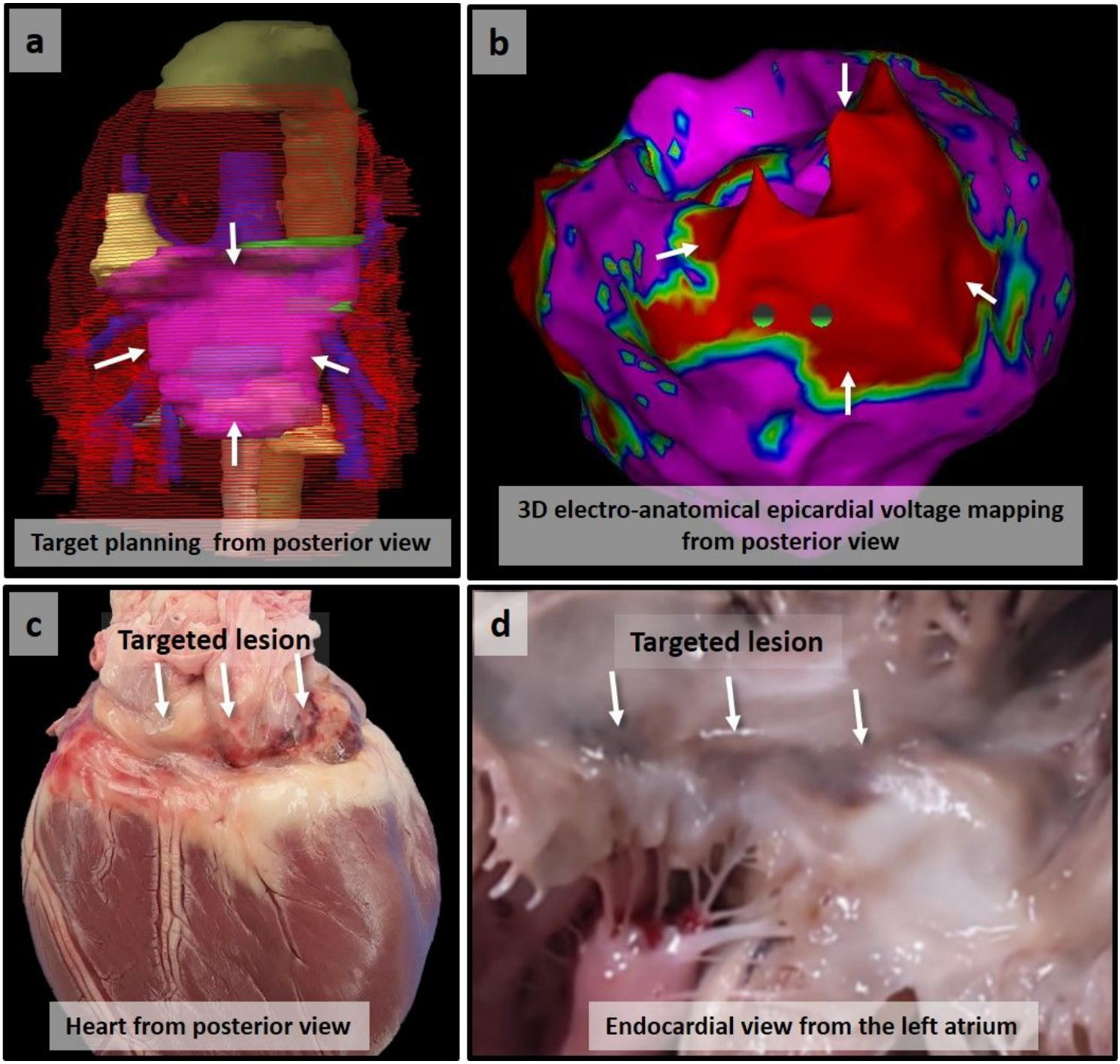

Figure 3

Myocardial necrotic scar formation on irradiated left atrial posterior wall. The reconstructed target area from the posterior view (white arrows in a) corresponds with the low voltage area (red area with white arrows in b) indicating a scarred lesion on voltage mapping with the CARTO-3 electroanatomical mapping system (Biosense Webster Inc.). The targeted lesion is grossly distinguishable at 4 months from both the epicardial (c) and endocardial (d) side.

Figure 4

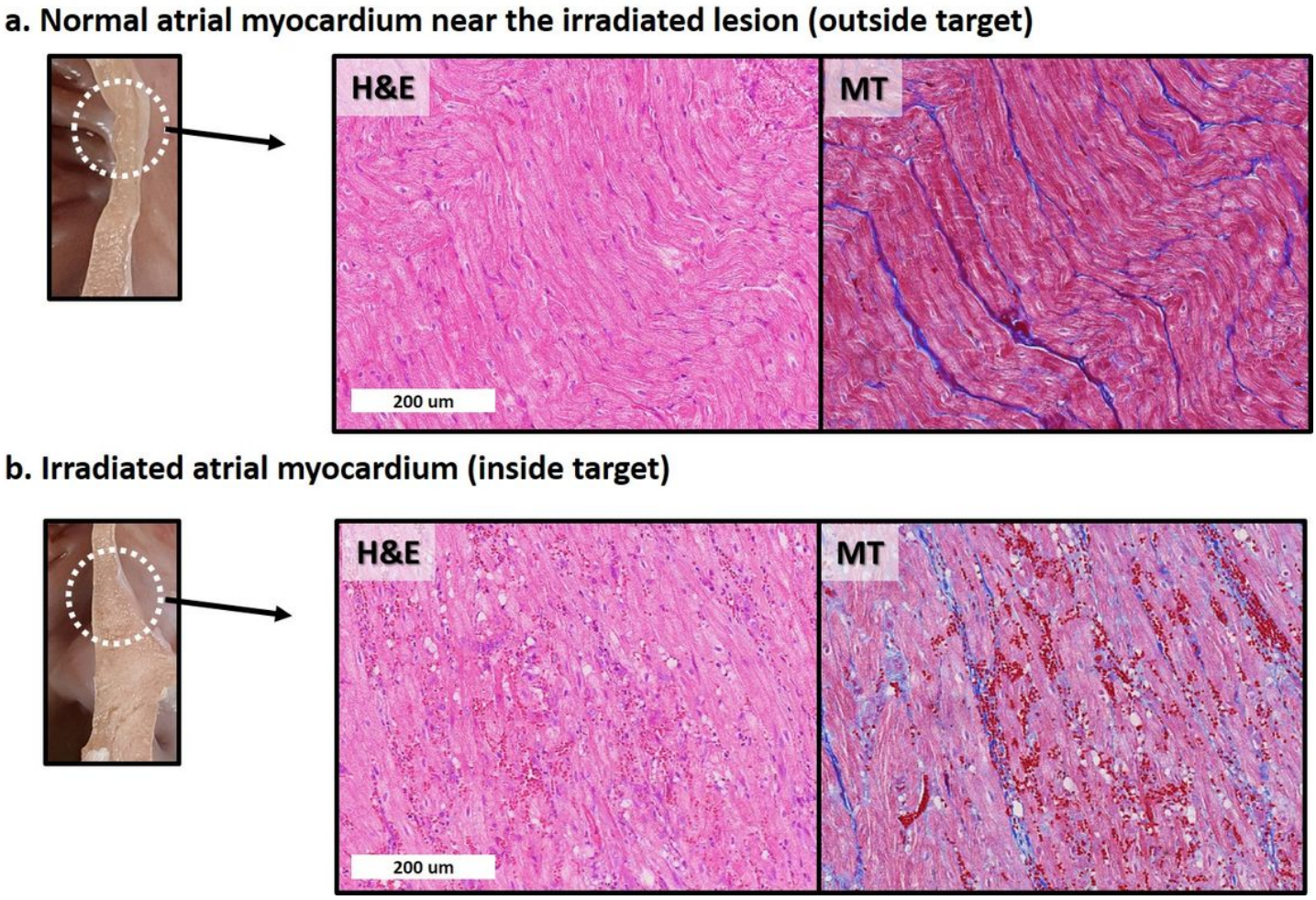

Figure 4

Histologic changes after irradiation at 6 weeks. There is no gross lesion at 6 weeks. However, from the light microscopic evaluation with H&E and MT staining, compared to normal atrial myocardium near the irradiated lesion (a), irradiated atrial myocardium (b) shows diffuse vacuolization with extensive hemorrhage and inflammatory cell infiltration with dilated capillaries. H&E, hematoxylin and eosin; MT, Masson's trichrome

Figure 5

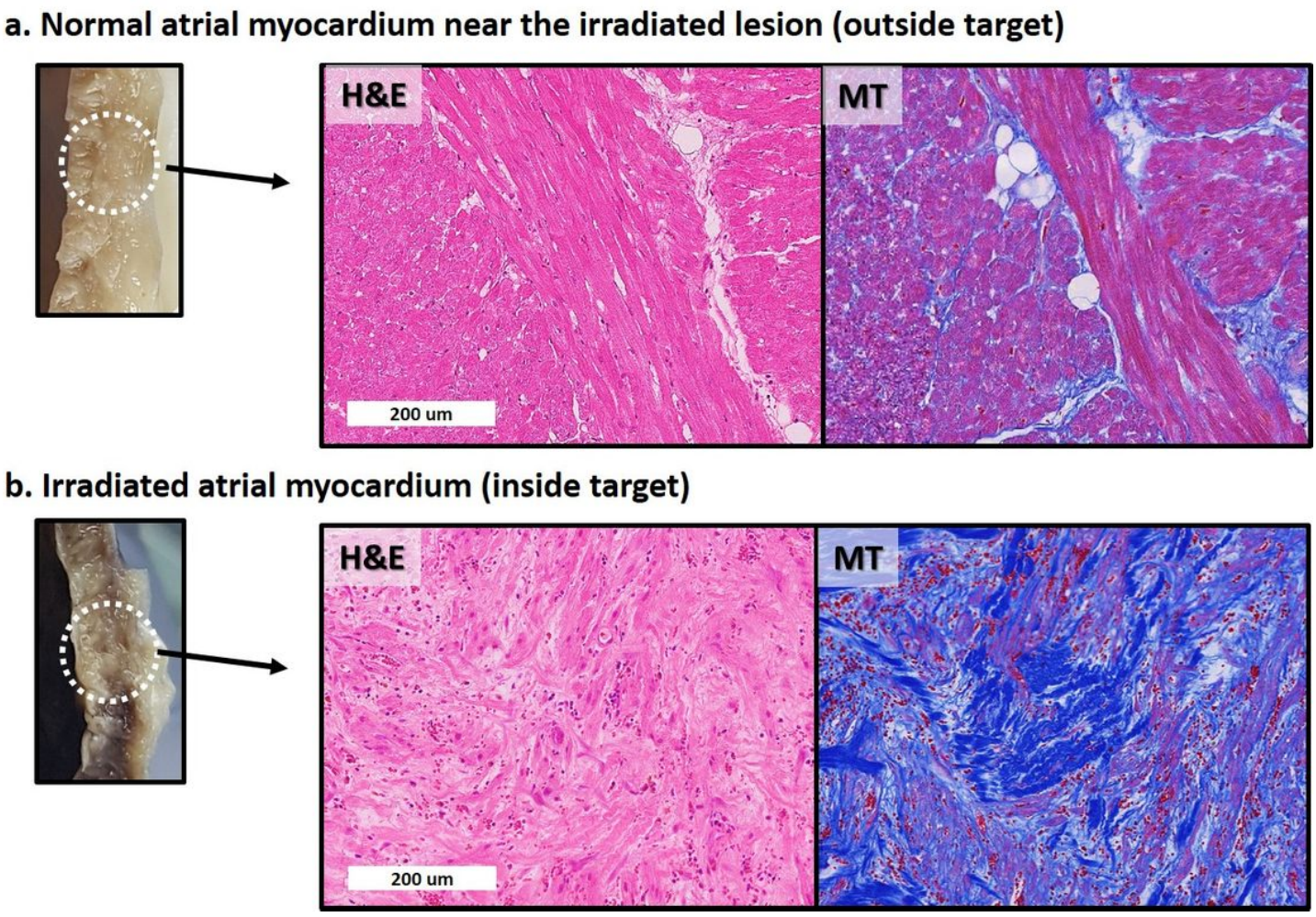

Figure 5

Histologic changes after irradiation observed at 4 months. A visually definite transmural necrotic lesion is observed on the irradiated area at 4 months. Compared to the normal atrial myocardium near the irradiated lesion (a), irradiated atrial myocardium (b) shows massive hemorrhage with anucleated wavy fibers with extensive interstitial fibrosis. H&E, hematoxylin and eosin; MT, Masson's trichrome

Supplementary Files

This is a list of supplementary files associated with this preprint. Click to download.

- SUPPLEMENTARYMATERIALS.pdf